Measurement of Thin Liquid Film Characteristics using Laser Focus Displacement Instruments for Atomization Applications

J. L. Wegener*
Department of Mechanical and Aerospace Engineering
University of California - Los Angeles
Los Angeles, CA 90095-1597 USA

J. A. Drallmeier
Department of Mechanical and Aerospace Engineering
Missouri University of Science and Technology
Rolla, MO 65409-0050 USA

Abstract

Dynamic thin liquid films are present in numerous engineering applications including atomizers, wave plate mist eliminators, and refrigerant flows in evaporators. As computational models emerge and evolve to describe the complex behavior of such films, experimentalists search for robust methods for validating these models. An experimental film thickness measurement technique is one example of the desired methods, and here a laser focus displacement instrument (LFD) is explored as a solution. An LFD utilizes the confocal principle with laser light to determine the location of an interface between two media. The device has seen use in static applications such as product quality verification processes where spatial accuracy is paramount, and a limited few research groups have applied an LFD to fluid dynamics applications such as would be encountered in atomization processes. Although researchers had success using the instrument as a film thickness measurement technique, there lacks a comprehensive study of the technology's capabilities when used as such. This study examines the abilities of the LFD technology by isolating and quantifying its limitations, including optical configuration as well as fluid properties such as refractive index. Following a detailed description of the instrument, theoretical calculations and static liquid experiments were performed to identify the maximum surface angle which allows measurement. This limitation is important for wavy liquid film applications. The surface angle limitation, combined with temporal resolution, will largely determine whether a time-resolved film surface profile can be obtained or if only time-averaged film thickness measurements are possible. An LFD was applied to both gravity driven films and shear-driven films to show the significance of film surface dynamics and experimental thickness measurements are presented for both cases. The experimental results and analysis show that the specific model of LFD utilized in this study can provide accurate time-averaged measurements for shear-driven films, but only with explicit changes in instrument specifications can the instrument provide time-resolved shear-driven film surface profiles.

Key words: laser focus displacement instrument, film thickness, film surface angle

*Corresponding Author: jwegener@ucla.edu

Introduction

Thin liquid films are found within a wide array of industrial applications, and many of these applications have been subject to detailed investigation. Atomizers, wave plate mist eliminators, and refrigerant flows in evaporators have been investigated by experimentalists aiming to create and/or validate theoretical models which predict the behavior of liquid films [1,2]. It is clear that film atomization, and the events which lead to film atomization, are highly dependent on the characteristics of liquid film and adjacent gas flow. Film thickness, among other characteristics, will greatly influence the degree of atomization which occurs and has consequently become a crucial measurement for experimentalists in the atomization field.

Thus, the demand for robust film thickness measurement techniques has driven the development of a number of methods. These methods are often based in the realms of electricity or optics. For a long time, needle contact methods and fluid conductance methods were the most popular modes of measuring film thickness, as discussed by Hewitt [3]. But, these techniques are intrusive to film behavior due to the needle contact point on the film surface or the meniscus formation at the wire-film interface in the case of conductance methods. As a result, a generation of non-intrusive film measurement techniques developed. This series of techniques is based in the field of optics. Fundamental knowledge of light absorption and reflection coupled with innovations in lasers and imaging technology has been used to develop several non-intrusive thickness measurement techniques.

The studies which document these developments are often focused not only on a film thickness measurement technique, but instead the paramount focus is a fluid dynamics problem which requires subsequent film thickness measurement. As a result, many different techniques emerged with their own desired capabilities or lack thereof, with each technique tailored for a particular experimental environment. Temporal resolution, spatial resolution, geometry, fluid species, and other specifications were appropriated by investigators to fulfill certain requirements for each experimental situation. The resulting array of methods lacks a universal, robust technique which can be applied without expertise in optical or electrical diagnostics.

The laser focus displacement (LFD) instrument has emerged as a possible solution. A laser focus displacement instrument utilizes the confocal principle with laser light to determine the location of an interface between two media. By moving the focal point of a converging laser beam, the LFD instrument locates a surface by sensing peaks in reflected light intensity when the laser's focal point is at the interface of two media. This technology is most widely utilized in product testing and product quality verification that requires fine surface finishes or material thickness. Originally developed for detecting scratches on electrical devices, the LFD is also used in applications such as measuring a brake disc surface profile, measuring glass thickness, and measuring the thickness of a contact lens in the plastic industry.

Within the LFD measuring unit, a semiconductor laser source produces an unpolarized, diverging beam of light as shown in the diagram in Figure 1. A collimating lens then precedes an objective lens, which causes the beam to converge to a point at a known location. The focal point is moved up and down by moving the objective lens in an oscillating manner. This is achieved by constraining the collimating lens to a known location and securing the objective lens on one of the vibrating prongs of a tuning fork. The tuning fork is then subject to a known frequency from a vibration source and in turn, the objective lens oscillates at a known frequency and amplitude. The focal point of the beam scans up and down at the same frequency and amplitude as the objective lens. When the focal point is located on the target surface, then the light will be reflected back into the LFD measuring unit with greatest intensity. When light passes through the pinhole shown in Figure 1, the light receiving element senses a light intensity peak. With a known location of the oscillating objective lens measured by a position detection sensor, the LFD can match the light intensity peak with a focal point location. Thus, the target surface location can be determined.

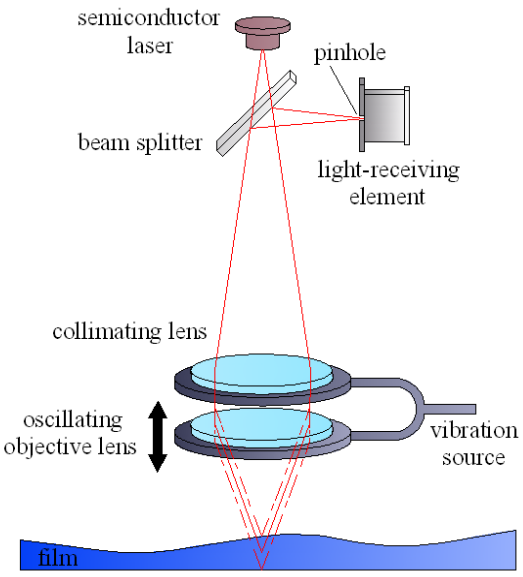

Figure 1. Laser focus displacement measuring unit diagram.

Background

Takamasa and Kobayashi [4] were the first to use an LFD for liquid films. Their study applied the instrument to annular two phase flow of films inside a vertical, transparent tube. An LFD instrument manufactured by Keyence Co., Model LT-8100 was used, which provided spatial resolution of 0.2 μm and temporal resolution of 0.7 kHz. Spatial resolution is defined here by the minimum change in surface height that could be detected. The LFD was mounted outside the vertical circular tube, and the thickness data provided by the LFD was used to calculate wave amplitude, wave frequency, maximum film thickness, minimum film thickness, and average film thickness. Takamasa and Hazuku [5] then expanded the use of this technique by using two LFDs simultaneously, showcasing the instrument's applicability.

Busam et al. [6] utilized laser focus displacement technology for film thickness measurements in an aero-engine system where oil is used to lubricate bearings. An observation was made concerning the film surface angle limitations of the LFD. It was estimated that only waves with a maximum slope of about $\theta_c/2$ between the surface and the optical axis of the sensor can be detected, where θ_c is the cone angle of the incident laser beam. For the instrument LFD model used by Busam et al. [6] the cone angle was 23˚, but the study did not present experimental verification confirming a limitation of 11.5º. Instead, it was stated that with respect to highly viscous flows the maximum slope is great enough to avoid impacting the resolution of the wave structure. Hazuku and Fukamachi [7] used an experimental test to determine the maximum measurable surface angle when glass is the subject piece. In this test, an LFD was used to measure the location of the outside surface of a glass tube. If the LFD is centered on the tube, then the surface angle is zero degrees in relation to the laser beam axis, but if the LFD traverses across the tube then the surface angle increases in relation to the laser beam axis. The maximum measurable surface angle of the glass tube was 33°, different than the prediction of Busam et al. [6]. The LFD model used in Hazuku and Fukamachi [7] utilized a greater cone angle, θ_c = 43.4º. This value is much greater than that in [6], which should provide for a greater maximum measurable slope according the limiting $\theta_c/2$ criterion. But, although θ_c = 43.4º indeed provided a greater maximum measurable surface angle, 33º is even greater than half the cone angle. The discrepancy revealed by observing this pair of studies raises questions regarding other factors which may influence the angle limitation. Laser beam cone angle appears to be one component of a broader optics problem which requires further study.

Hazuku et al. [8, 9] has performed recent studies using an LFD to measure films in annular two phase flow. In [8] the mean film thickness was used to calculate a one-dimensional interfacial area concentration. A comparison was made between the interfacial area concentration from measured data and the interfacial area concentration calculated using a computational model for annular-mist flow. In [9] the LFD was applied to shear-driven annular flow in a vertical glass pipe 5 mm in diameter. Recorded film thicknesses ranged from 100 μm to 900 μm, and mean film thickness and disturbance waves were studied. High speed imaging was combined with the LFD's measurements, and the images showing large and small film thicknesses correlate well with LFD measurements taken simultaneously.

Scope

This study examines the abilities of the LFD technology as a fluid dynamics tool. Fluids experimentation offers the technology a measuring environment more demanding than the conventional applications of LFD technology. Liquid film thickness measurements can be performed with a LFD instrument as shown by recent studies ([4-9]), but when such measurements are performed with rapidly changing film thicknesses and steep surface angles, the limitations of the device are noticeable. These limitations will be defined with emphasis on the surface angle limitation, which will be investigated using both theoretical and experimental methods. The theoretical portion will examine material reflectivity and geometric calculations. The experimental portion will examine static liquid and solid thickness measurements, gravity-driven film measurements, and shear-driven film measurements.

Surface Angle Limitations

The LFD technology is limited by the surface angle of the interface. The surface angle must be small in order for the light receiving element to detect a light intensity peak. Large surface angles cause reflected light to scatter instead of reflect back into the measuring unit to be detected by the light receiving element. The maximum possible surface angle estimated by Busam et al. [6] and experimentally measured by Hazuku and Fukamachi [7] and provide the only two estimates concerning the maximum measurable surface angle of a given subject.

In this study, a more detailed examination of surface limitations will be presented by quantifying measurability of the top and bottom surface both theoretically and experimentally to develop a methodology for establishing an angle limiting criteria. In the case of both top and bottom surface

measurements, the subject material and the surface angle will influence the amount of light that is reflected or refracted at the interface. As a result, theoretical calculations are made investigating both surface angle and subject material influences. These calculations include geometric calculations for top surface reflection followed by bottom surface reflection. Then, material reflectivity influences will be introduced as an important factor in surface measurability.

An important point needs to be made relative to the the two methods that could be used to measure the thickness of a film on a solid substrate using an LFD. The first method includes measuring the top and bottom interface locations simultaneously (e.g. the air-liquid interface and the liquid-solid interface). The second method is to detect the solid interface without liquid present, measuring only the air-liquid interface while assuming the lower substrate does not move relative to the instrument. Both methods will be investigated here, but the results will illustrate distinct disadvantages of the first method.

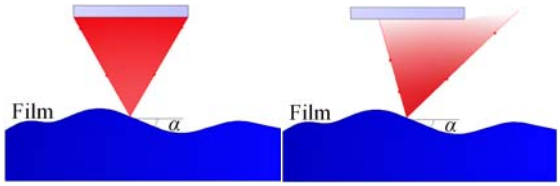

(a) (b)

Figure 2. (a) Path of incident laser beam. (b) Path of reflected laser beam.

First, calculations predicting the maximum surface angle for measuring the location of the top surface were made. Figure 2 shows the path of light resulting from top surface reflection, where the surface angle, α, is measured from the horizontal. The reflected light projects an illuminated circle onto the objective lens, and as α changes, the location and shape of this projected area changes as well. As α deviates from zero, the reflected laser cone projects an ellipse shape on the objective lens rather than a circle. As α increases, the center of the projected ellipse moves farther from the original center of the laser beam, resulting in an illuminated area represented in Figure 3. As α increases, a decrease in the amount of light reflected back through the objective lens inhibits the LFD light sensing element's ability to detect the light intensity peaks necessary to measure the target surface. It is important to note that for simplicity, it is assumed the light receiving element will detect light if the path of reflected light overlaps the original path of the incident light. Although the receiving element's aperture may not provide a condition for detecting all reflected light at $\alpha = 0$, a method which offers a consistent relative approximation will account for these losses throughout the entire range of surface angles. Therefore, the light receiving element's aperture size is not used in this study. Instead, a relative area calculation is used to accommodate for losses due to an increase in surface angle, normalizing aperture effects.

Calculations were performed to study the amount of light reflected over the original path of incident light. Using integral calculus for the functions of a circle and an ellipse, the area of the intersecting region A in Figure 3 was calculated as a function of α and related to $A(0°)$, where $A(0°)=\pi R^2$. R is the radius of the circle shown in Figure 3. Figure 4 shows $A(\alpha)/A(0°)$ plotted versus α/θ_c, which presents large changes in $A(\alpha)/A(0°)$ as α/θ_c deviates from zero.

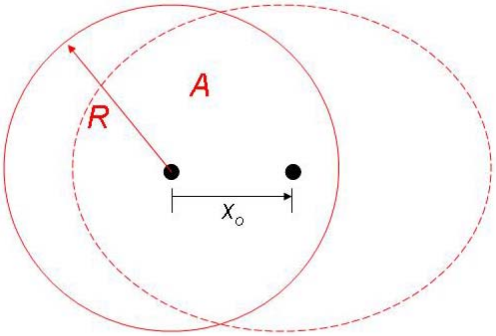

Figure 3. Projected area of light due to top surface reflection as viewed from above the objective lens.

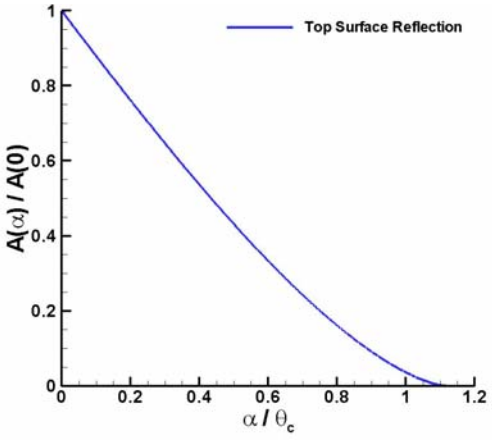

Figure 4. Relative area of the reflected light from top surface reflection plotted versus surface angle.

To investigate the angle limitations for the measurability of the bottom surface, further theoretical calculations were performed. To appropriately address the case of liquid film measurements where the top surface is an air-fluid interface and the bottom surface is a static fluid-solid interface, calculations utilize a variable top surface angle and a constant bottom surface angle of 0°. This addresses cases where a liquid film flows over a solid substrate which has a flat surface perpendicular to the path of the laser.

This situation is represented in Figure 5, which shows the refraction of light at the air-fluid interface. Note that as α increases the reflected light is projected further to the left, whereas in Figure 2 the opposite trend is shown. Theoretical predictions of the maximum top surface angle for measuring the bottom surface required knowledge of the measuring unit geometry, subject thickness, and the subject material's refractive index. These calculations are similar to those performed for top surface predictions, but must account for the refraction of light passing through the subject material. Once again, the proportion of light reflected over the path of incident light is of interest because it is assumed the reflected light must propagate over the incident beam path to be captured by the light receiving element. Similar to the methods described above, the area of the intersecting region A was calculated as a function of α. Similar to Figure 4, Figure 6 shows $A(\alpha)/A(0°)$ versus α/θ_c. Figures 4 and 6 depict similar trends, but Figure 6 includes $A(\alpha)/A(0°)$ values for three different refractive indexes in order to show the influence material has on refraction geometry. When water is used the reflected laser's projected area overlapping onto the path of incident light is almost equal when comparing bottom surface reflection to top surface reflection. Figure 6 also shows that refractive index has a significant effect on the area of reflected light. A subject material with a large refractive index will cause surface angle to have a greater influence on the amount of reflected light.

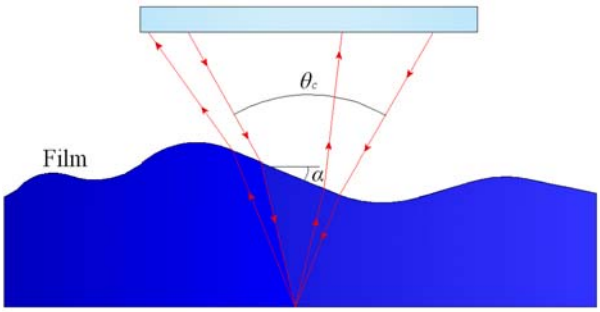

Figure 5. Bottom surface reflection diagram.

The influence of subject thickness on bottom surface reflection was also investigated. For all three refractive index values shown in Figure 6, $A(\alpha)/A(0°)$ was calculated for thicknesses of 0.5 mm, 1.0 mm, and 2.0 mm. This range of values represents common thicknesses for dynamic film studies [1,10], and changes in $A(\alpha)/A(0°)$ within this range were negligible. This occurred partly due to the subject thickness being much smaller than the focal length of the objective lens, which was 20 mm for the instrument used here. Thus, thickness variation was not given further consideration for this study.

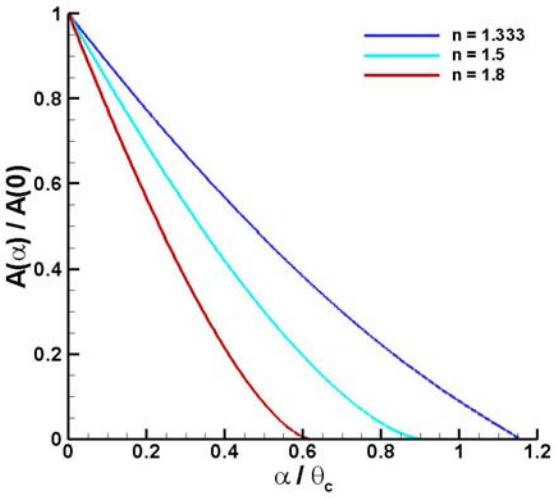

Figure 6. The relative area of the reflected light from bottom surface reflection plotted versus surface angle.

Area calculations approach the problem strictly from a geometric outlook. The physics of light propagation must include more factors and make viable assumptions where possible. For example, a laser beam's intensity is not evenly distributed throughout the beam. Light is concentrated in the center and weaker intensities exist near the beam's perimeter. Also, light will be transmitted and absorbed at an interface, causing decreases in the amount of reflected light. In conclusion, geometric calculations should not stand alone in this analysis.

The relative area calculations can be used in part to establish a more appropriate parameter. The relative power, P/P_o, offers a more direct way to quantify the amount of light received by the light receiving element. P is the total power reflected into the LFD and P_o is the total power of incident light from the LFD. The total power (or flux) of a beam of light is a product of the cross sectional area of the beam and the mean intensity

of light throughout the beam, or the electric flux density per unit time [11]. Thus, P will be determined by the area of reflected light, $A(\alpha)$, and the intensity of light, I, which is variable throughout the laser beam. Since the intensity profile of the beam is unknown, values for P cannot be calculated, but an approximation of the P/P_o ratio can offer an estimate of how much of the incident light's power is received by the LFD. The recently discussed geometric calculations will provide an excellent starting point for predicting P/P_o as a function of α/θ_c.

The light intensity profile of a laser beam will vary when viewing several different individual lasers. Therefore, a more universal approach was applied here by assuming an evenly distributed beam intensity. This approach causes more light to be lost at small α because the perimeter of a beam contains significant power, whereas a Gaussian type beam profile will not lose significant power until the beam's center area is undetected.

Also, relative power calculations must include losses due to transmittance and absorbtion of light within the media. Such losses can be accounted for by the reflection coefficient. The reflection coefficient utilizes refractive index, polarity, and incident angle to determine a percentage of light which will reflect at a given interface.

A material that inherently reflects more light than other materials is expected to allow for higher limitations in surface angle, and in order to analyze this further, the reflection coefficient, ρ, was calculated for different materials at various surface angles. The reflected light intensity was then calculated as the product of the reflection coefficient and the incident light intensity.

To determine the reflection coefficient, one must consider a beam of light passing through the interface of two media. The Fresnel equations follow as

$$\rho_{\perp} = -\frac{\sin(\theta_1 - \theta_2)}{\sin(\theta_1 + \theta_2)} \tag{1}$$

$$\rho_{//} = \frac{\tan(\theta_1 - \theta_2)}{\tan(\theta_1 + \theta_2)} \tag{2}$$

where θ_1 is the angle of incident of light relative to the optical axis, θ_2 is the angle of refracted light relative to the optical axis, $\rho\perp$ is the reflection coefficient for light polarized with the electric field of light perpendicular to the plane of propagation, and $\rho_{//}$ is the reflection coefficient for light polarized with the electric field of light parallel to the plane of propagation.

For unpolarized light, the reflection coefficient, ρ, was then appropriately calculated as the average of $\rho\perp$ and $\rho_{//}$,

$$\rho = \frac{\rho_{\perp} + \rho_{//}}{2} \quad . \tag{3}$$

To research the influence of the incident angle, θ_1, it was determined that increasing the incident angle from 0° to 10° caused a 0.05% increase in the reflection coefficient for water in air (n_w=1.333), 0.04% for optical crown glass in air (n_o=1.5198), and 0.03% for sapphire in air (n_s=1.7644). The trends of the reflection coefficient for metals are also of interest, because the solid substrate beneath liquid films often consists of metals. For electrically conductive materials, such as aluminum, the refractive index contains an imaginary part, k, where

$$m = n(1 - ik) \quad . \tag{4}$$

For example, when Snell's Law is applied to the case of light crossing the interface of a dielectric medium and a conductive medium the imaginary component of the refractive index causes Snell's Law to follow as

$$n_1 \sin\theta_1 = m_2 \sin\theta_2 = n_2(1 - ik_2)\sin\theta_2 \tag{5}$$

where n_1 is the refractive index of the dielectric medium and m_2 includes the real refractive index of the conductive medium, n_2, and the imaginary part, k_2. A different form of the Fresnel equations must be utilized to include the imaginary part of a material's refractive index [12]. Proceeding with n_a=1.44 and k_a=3.694 for aluminum, the Fresnel equations reveal a 0.002% change in the reflection coefficient for aluminum in water when incident angle changes from 0° to 10°. Thus, after observing these calculations for various materials, it was concluded that the change in reflected light intensity due to a change in surface angle is negligible over the range of expected surface angles. But, regardless of θ_1, changes in material manifest a notable change in the reflection coefficient. At θ_1=0° the reflection coefficient of water, optical crown glass, and sapphire in air is 0.0205, 0.0424, and 0.0762, respectively. The reflection coefficient of aluminum in water is 0.7870. Such changes in ρ were used within the theoretical predictions of surface angle limitations, because it is expected to observe increasing surface angle limitations with an increasing reflection coefficient due to a loss in reflected power.

Using the preceding concepts regarding the reflection coefficient, the relative power, P/P_o, was determined with losses at the air-water interface and the water-

aluminum interface below the film. For top surface measurements of water the $A(\alpha)/A(0°)$ values shown by Figure 4 were multiplied by ρ_w to give the result shown by Figure 7. Due to the small reflection coefficient of a water-air interface (ρ_w=0.0205), Figure 7 shows a significantly lower power for the top surface reflection. In the case of bottom surface reflection, the larger reflection coefficient for the aluminum-water interface will have a less significant effect on P/P_o. Examining the Fresnel equations shows that 78.7% of light is reflected at the water-aluminum interface. When making bottom surface measurements though, light must travel from the LFD instrument through the air-water interface, reflect off the water-aluminum interface, and then travel through the water-air interface to reach the LFD. Therefore, the retained light intensity decreases at each of these three interfaces. As a result, calculations showed 75.6% of the original light intensity is retained when measuring the water-aluminum interface beneath a film. Since the amount of light lost due to absorption is negligible, a reflection coefficient of 0.756 was used to include the reflection properties of each interface.

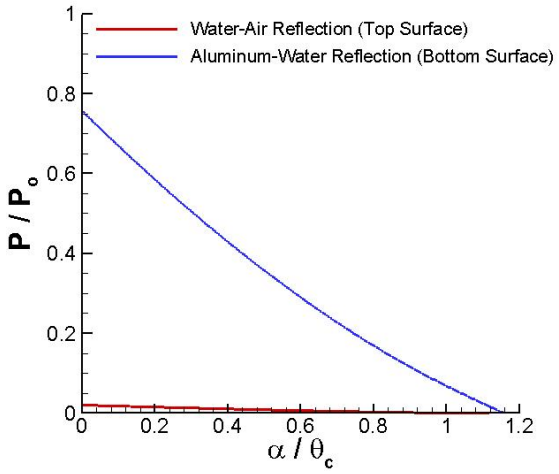

Figure 7. The relative power with top surface reflection of a water-air interface and with bottom surface reflection of an aluminum-water interface.

In order to use these relations for predicting the maximum surface angle allowing measurements, a minimum relative power value is needed. A baseline number can provide a threshold representing the minimum amount of incident light needed for the LFD to detect an interface. If this threshold is known then the maximum surface angle allowing measurements can be determined by finding α/θ_c at the point where relative power is equal to the threshold value. To establish this threshold, or minimum relative power, experiments were conducted to find the maximum surface angle allowing measurements in a static, controlled situation. The maximum angle determined from these experiments was used in conjunction with the previously discussed P/P_o versus α/θ_c calculations in order to find the minimum relative power.

Experiments

This study utilized a Keyence laser focus displacement instrument, model LT-9030. Measurement range, which is the total vertical movement of the focal point, is 2.0 mm for the LT-9030. The spatial thickness resolution is 0.1 μm and the spot diameter of the laser beam focal point is 7 μm. The cone angle, θ_c, is 23°. The sampling frequency of the LFD is 1.5625 kHz, which corresponds to a cycle time of 0.640 ms. This speed is not fully realized in data collection due to the reset time of the LFD controller, which is 3 times the raw cycle time. Including the reset time results in a cycle time of 1.92 ms and a frequency of 520.83 Hz.

The system described above was used in an array of experiments to explore its ability to measure flat surfaces held at an angle. The measurement of solid surfaces held at an angle is first discussed. Then, after establishing several fundamental concepts from glass and sapphire surfaces, measurements are applied to static liquids with a curved surface. This methodology will allow conclusions to be drawn from experiments where thickness, refractive index, and surface angle are known with high accuracy before testing the instrument's ability with liquids, where thickness and surface angle are to be determined by the experiment itself.

Static Solid Thickness Measurements

Optical crown glass with a thickness of 0.2 mm along with sapphire disks with thicknesses of 0.508 mm, 1.016 mm, and 2.032 mm were used as the subject pieces in order to isolate thickness and refractive index effects. For each subject piece, displacement measurements were recorded for three different locations on the top surface while controlling the angle of orientation, α, on an adjustable stage with an uncertainty of ±0.2°. The LFD mounting apparatus positioned the measuring unit vertically with an uncertainty of ±0.1˚.

The resulting maximum measurable angle was 8° for each of the subject pieces, with the exception of the 1.016 mm sapphire disk, which was measurable at 8.5°. It was found that the maximum angle was dictated by a near complete loss of a measurable reflected signal which occurred rapidly over a small surface angle

change near the angle limit. The deviation of the measured thickness to the measured mean thickness of each subject is shown in Figure 8. The standard deviation for each set point was calculated as

$$\sigma = \sqrt{\sum \frac{\left(h - \bar{h}\right)^2}{n}} \tag{6}$$

where σ is standard deviation in microns, h is measured thickness in microns, $\bar{h}$ is mean measured thickness in microns, and n is the total number of measured values. Standard deviation in the time sampled results are shown to illustrate the impact of noise in the measurement which begins to have a larger effect at steep angles. Note the standard deviation of each measurement remains within 1% of the actual thickness until the maximum limit is reached. Additionally, measurements show the average thickness remains within 2% of the actual thickness despite this increase in noise at larger angles. This is shown in Figure 9, where error is the difference between mean measured thickness, $\bar{h}$, and the actual thickness.

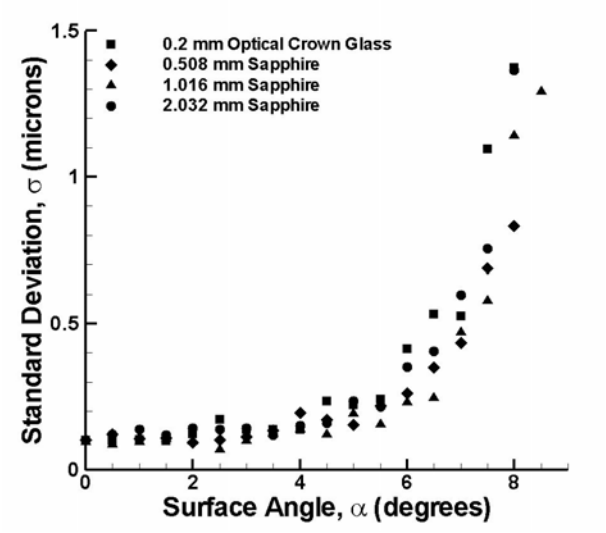

Figure 8. Thickness measurement standard deviation for four subjects for various angles of orientation.

Therefore, although the LFD was less precise at high α, the mean thickness values remained accurate until the maximum surface angle allowing measurement was reached. The maximum α for sapphire was 8.5±0.55° for top surface reflection, which corresponds to α/θ_c=0.370±0.024. The maximum α for optical crown glass was 8.0±0.55° for top surface reflection, which corresponds to α/θ_c=0.348±0.024. The bottom surface of these specimens was parallel to the top surface and such geometry is uncommon in dynamic film studies. As a result, only the maximum angle allowing measurement of the top surface was used from the sapphire and optical crown glass data.

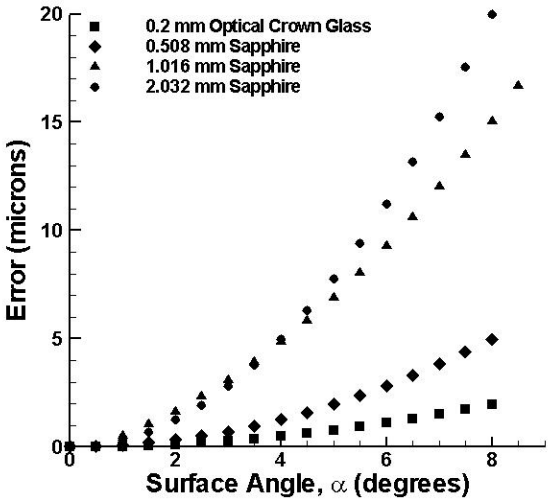

Figure 9. Thickness measurement error calculated as the difference between mean measured thickness and actual thickness.

To relate such results with the theoretical calculations of this study, a P/P_o versus α/θ_c plot was created for optical crown glass and sapphire (n_o=1.5198, n_s=1.7644). Figure 10 presents this plot with points representing the measured threshhold angle as established by experiments. The α/θ_c values can then be used to estimate a minimum power requirement. The maximum measurable surface angle will change due to a change in a specimen's refractive index or the laser beam cone angle, but a minimum power value offers a baseline for comparison with any given set of characteristics. In Figure 10, points for optical crown glass (0.348, 0.021) and for sapphire (0.370, 0.020) were used to create a minimum relative power value of 0.021 shown by the dashed horizontal line. Thus, the minimum relative power needed for an interface to be detected by the LFD was predicted to be only 2.1% of the incident light's power, P_o. Therefore, a small proportion of the incident light must be received by the light receiving element in order to detect an interface. Employing this methodology with liquids will better explore its applicability to atomization applications.

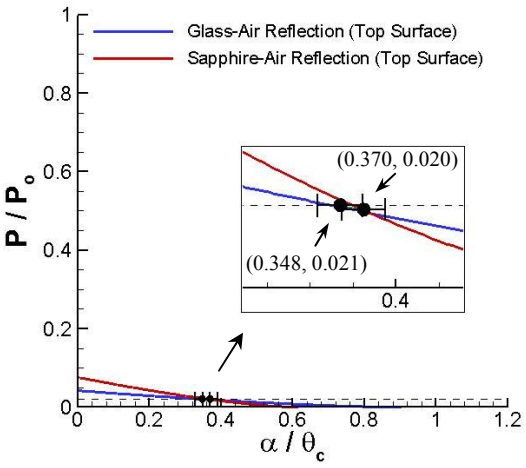

Figure 10. Relative power versus surface angle divided by laser cone angle. The estimated minimum power is shown, including points representing the maximum measurable angle.

Static Liquid Displacement Measurements.

To investigate an LFD instrument's capabilities for a liquid-gas interface, a static liquid bubble was used as the subject. The objective was to find the maximum measureable surface angle as in the experiments for glass and sapphire described above. Surface location measurements were made for a 50 µL drop of water-surfactant mixture placed on a flat, polished aluminum plate. This created a liquid bubble as shown by the image in Figure 11. The surfactant was used to develop varying drop thickness and had negligible impact of the refractive index of the liquid. The aluminum surface is secured at 0˚ from the horizontal with an uncertainty of ±0.5˚. The surface angle of this bubble relative to the horizontal is largest at the outside edges of the fluid and smallest at the apex in the center, which results in areas near the perimeter of the bubble where the surface angle is too large for measuring. In making such measurements, the laser focal point traveled from the edge towards the center of the fluid and then continued towards the opposite edge of the fluid. The first data point was recorded at the first measurable location. The last data point was recorded at the last measurable location.

Two-dimensional image analysis was used to find the surface angle at the limits of measurement. A photo of each liquid bubble was studied using an image analysis algorithm which used the raw image to create a sixth order polynomial function representing the surface profile of the liquid bubble. By finding the derivative of the fitted polynomial function, the surface angle was determined for all locations. For each repetition of this process one pixel represents approximately 60 µm, which results in an uncertainty of ±30 µm when converting spatial units from image pixels to microns. During the time passed during the measuring process, the liquid bubble partially evaporated which changed the height of the bubble without changing the location of the edge of the bubble. To address this dilemma, photos were taken immediately before and after the measuring process. This provided one image for left side calculations and one image for right side calculations, where the bubble has decreased in size during the measurement process.

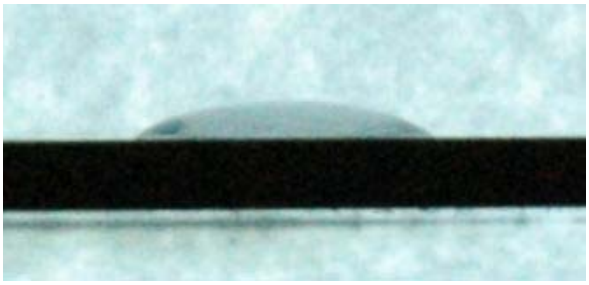

Figure 11. 50 µL of 0.1% surfactant mixture placed on a polished aluminum surface.

In order to experimentally validate the maximum surface angle for measuring the bottom surface, the same 50 µL liquid bubble method was used. Similar to the previously mentioned top surface measurements, surface location data for the aluminum-water interface was attained where the interface was detected by the measuring unit. Although the target surface, the aluminum-water interface, was oriented such that α=0°, a large water-air surface angle prevented detection of a portion of the horizontal aluminum-water interface. This situation arises when the light passing through the water-air interface is refracted at a large angle, causing light which reflects off the aluminum surface to scatter away from the measuring unit instead of reflect into the light sensing element as desired. Thus, similar to measuring the water-air interface, there was a small area near the perimeter of the bubble where the target surface was undetected due to the large angle of the water-air interface. But, the refraction of light passing through liquid also causes a shift in the measured location of the aluminum surface, creating an inaccurate result. Therefore, two problems exist. First, the instrument is unable to measure near the perimeter due to large surface angle. Second, the instrument provides an inaccurate location of the substrate surface resulting from refraction of light at the gas-liquid interface. Unfortunately a correction cannot be applied directly as

the surface angle is not know a-priori in most film measurements.

An example of the results is presented in Figure 12, where a 0.1% surfactant sample is shown. In finding the maximum surface angle, the derivative of the fitted polynomial equation was used for the first and last data points. For example, the calculated results for the 0.1% surfactant sample in Figure 12 were α=6.23° at the left limit of the profile and α=6.28° at the right limit of the profile. The complete procedure was repeated for both the 0.1% and 1.0% surfactant samples. The mean maximum angle allowing detection was 6.38° for 0.1% surfactant mixtures and 5.47° for 1.0% surfactant mixtures.

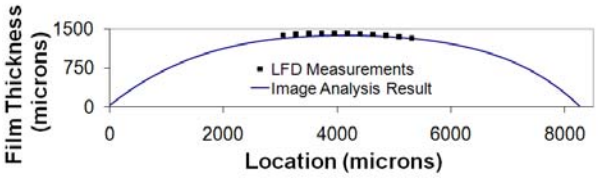

Figure 12. LFD measurements of a water-air interface plotted with results from liquid bubble image analysis. (0.1% surfactant mixture)

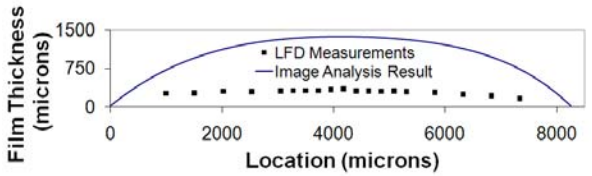

Figure 13. LFD measurements of an aluminum-water interface plotted with results from liquid bubble image analysis. (0.1% surfactant mixture)

Due to the ability of the LT-9030 model to measure two surfaces within each oscillation cycle of the objective lens, the surface data shown in Figure 12 is for the same liquid bubble as that which is shown in Figure 13. Figure 13 simply includes displacement data of the bottom surface instead of the top surface. Clearly these results show the apparent displacement of the bottom surface due to refraction through the liquid is significant (one-fourth to one-half of the film thickness). As this displacement is a function of the refractive index of the liquid, the top surface angle and the film thickness, correction of the results to estimate the film thickness would be non-trivial. Hence it is concluded that the only viable means by which to use the LFD to measure the thickness of a film with surface waves is to measure the film surface location and reference that to the know location of the substrate surface.

Minimum Relative Power Prediction

The use of different surfactant mixtures resulted in different surface profiles, and these differences were expected and desired in order to attain a more robust experimental average. When averaging all angle measurements the mean maximum angle allowing detection of the water-air interface was 5.92° with a total uncertainty of ±1.3˚. Since the LT-9030 has a cone angle of 23°, these results correspond to α/θ_c=0.257±0.11 for top surface reflection.

The maximum angle results were compared to the relative power calculations, resulting in a minimum relative power value of 0.014 for top surface reflection. This value are represented by the intersection point shown in Figure 14. The minimum relative power prediction of 0.021 obtained from the solid interface study is also shown in Figure 14, represented by a dashed horizontal line. Comparing the estimated power requirement with the measured minimums for water-surfactant mixtures shows indeed, the 1.4% relative power requirement shown for top surface reflection is appropriate. It is befitting that the minimum power prediction formed from top surface measurements of glass and sapphire is comparable with top surface reflection for liquid. By changing from solids to liquids, we have simply altered the refractive index.

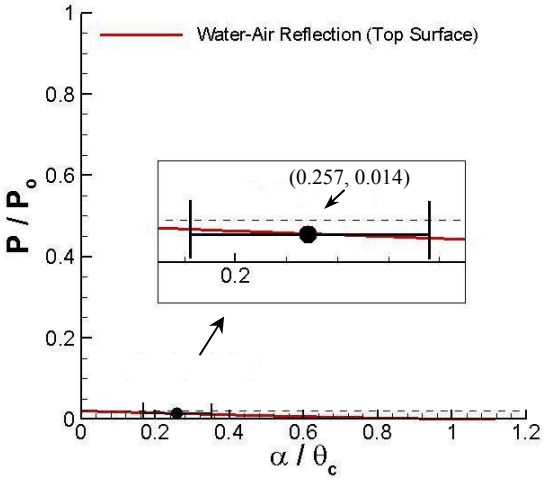

Figure 14. Relative power plotted versus surface angle divided by laser cone angle. The estimated minimum relative power is shown, including points of intersection.

The accuracy of a relative power prediction will greatly depend on the shape of the beam intensity profile. If nearly all of the laser's intensity is concentrated in the center of the beam then the maximum angle will be greater than if the laser's intensity is more evenly distributed throughout the radius of the beam. The function representing the beam intensity profile will greatly determine the shape of the P/P_o versus α/θ_c curve, and therefore, the validity of the minimum power prediction depends on the accuracy of the estimated P/P_o curves when compared to the actual P/P_o values determined by the actual beam intensity profile. However, the results for the top surface reflection using a variety of interfaces suggest that the maximum angle can be predicted by simply knowing the instruments cone angle and minimum detectable power ratio (~2% for the instrument used here).

In respect to other LFD studies, the results presented in Figures 10 and 14 introduce valuable new details. Busam et al. [6] previously stated that the maximum surface angle allowing measurement would be approximately $\theta_c/2$, while Hazuku and Fukamachi [7] experimentally determined α=33º for a model of LFD where θ_c=43.4º. Comparison shows disagreement between the two studies and neither study was reinforced by experiments presented here. An exception exists in the importance of laser cone angle, θ_c, which was emphasized by Busam et al. [6] and reinforced by this study's conclusions. The theoretical area calculations ameliorate this importance by revealing the relationship between α and θ_c, which justified a non-dimensional α/θ_c as the parameter of interest. This parameter combined with a relative power approach provides a more universal technique for estimating the surface angle limitation.

Application to Liquid Film Atomization

To better demonstrate the instrument's abilities as an atomization diagnostics tool a variety of experimental results was attained. As before, the Keyence LT-9030 LFD was used. The experimental facilities used for this portion of the study were built to initiate and control thin liquid film flow in an environment conducive for measuring film thickness, film width, and volumetric film flow rate. In the case of shear-driven films, the facility also measures gas flow rate, which is assumed zero in the gravity-driven film facility. The gravity-driven film facility is discussed in Lan et al. [13]. While details of the shear-driven film facility is given in Friedrich et al. [14].

Equipped with a better understanding of the instrument's limitations, applying the LFD instrument to dynamic films can reveal the ultimate effects of these limitations. The diverse flow conditions created by gravity-driven and shear-driven films offer a wide range of film surface angles. Gravity-driven films, with negligible gas phase flow, produce almost zero transient surface waves. Shear-driven films produce significant surface waves. Gas phase flow induces a shear stress at the film's surface, where a complex interaction of the gas and liquid flow creates a wavy surface. In this regime, the film surface angle is expected to range from zero to angles far greater than the maximum measurable surface angle. Concomitantly, if streamwise velocities are large enough to overcome the temporal resolution of the instrument then a second issue arises. Dynamic surface geometry can overcome the surface angle abilities of the instrument while the streamwise wave velocities overcome the temporal resolution. Such a situation can produce data similar to that shown in Figure 15, where a shear-driven film flow condition only slightly exceeded the angular and temporal abilities of an LFD instrument. Figure 15 shows approximate wave profiles. The steep sides of the surface waves and limited time resoultion of approximately 2 ms results in insufficient sampling to completely represent the surface profile. For the flow condition presented here the time resoultion of approximately 2 ms was not a limitation, but a flow condition with an increased wave frequency or increased film velcotiy can exceed the temporal abilities of the instrument. However, sufficient sampling can be obtained to determine a time-averaged film thickness as compared to other measurement methods [15].

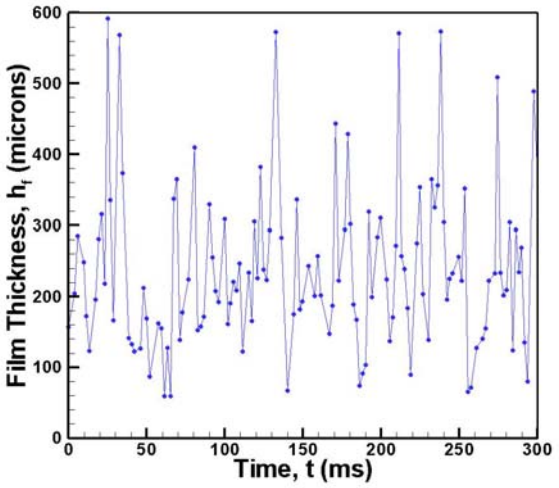

Figure 15. Time resolved shear-driven film thickness measured using a laser focus displacement instrument.

For both gravity and shear-driven experiments, thickness measurements took place far downstream from the film introduction point. The results then, were for fully developed film flow. The film width exhibits negligible transient changes, but the film thickness changes exist in the form of surface waves. Therefore, span-wise changes in surface angle generally occur near the outer edges of the film where surface tension acts to prevent fluid from spreading laterally. But, streamwise changes in surface angle occur in any location where transient waves exist. Consequently, as an LFD measuring unit moves from the outer edge of the film towards the span-wise center, the instrument will experience varying degrees of success.

For shear-driven film flow conditions similar to that shown in Figure 15, Figure 16 shows time-averaged film thickness results for a spanwise cross section. As discussed earlier, time-averaged LFD measurements offer accurate results although time-instantaneous surface profiles may not be measureable. For gravity-driven films, time-averaged data resembles that of shear-driven data. When comparing Figures 16 and 17, similar peaks in film thickness occur at the film edges while a minimum occurs near the span-wise center. The instrument was able to characterize a salient cross sectional thickness profiles for both shear-driven and gravity-driven cases.

Consequently, despite a clear difference in performance when acquiring time-resolved data for shear-driven and gravity-driven cases, time-averaged investigations are possible for both flow regimes.

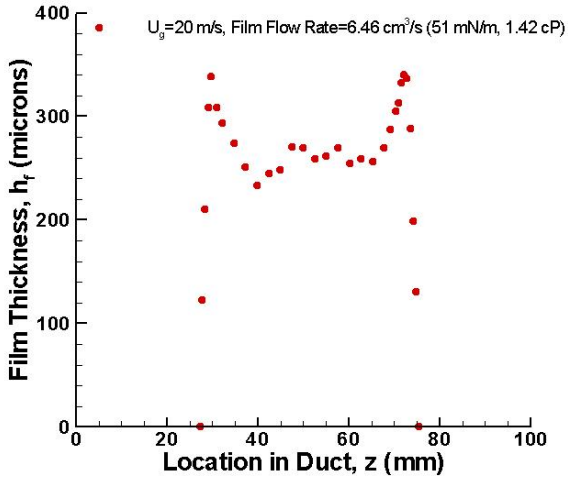

Figure 16. Time-averaged, spanwise, shear-driven film thickness profile.

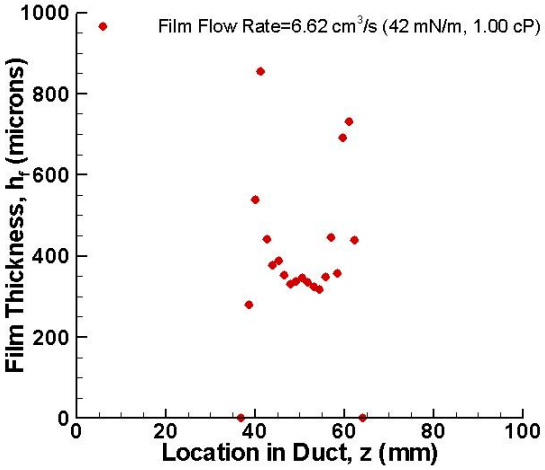

Figure 17. Time-averaged, spanwise, gravity-driven film thickness profile.

Conclusion

Previous studies exhibited the value of LFD technology as a fluid dynamics tool, but lacked a comprehensive definition of its limitations. One critical limitation is interface angle and warrants attention in applications involving curved liquid surfaces, constituting a large portion of atomizing applications. Although two previous studies have made valuable conclusions regarding a quantitative maximum measureable surface angle, this study used both theoretical and experimental approaches to encompass a broader array of factors.

With an understanding of the internal operations of an LFD measuring unit, theoretical work placed emphasis on amount of light which is sensed by the light receiving element after reflecting off the measured interface. In this manner, a power ratio which compares the reflected light to the incident light was calculated using geometrical calculations and material reflectivity. Then both solid and liquid specimens were used to find the maximum measurable surface angles in a variety of situations. Experimental and theoretical results were then merged to conclude that the instrument requires approximately 2% of incident laser light must be detected by the measuring unit in order to successfully measure the location of an interface. The use of Fresnel relations and knowing the liquid phase refractive index, provides a means to predict the maximum detectible surface angle for an instrument before measurements are made. The results also show that excellent measurement accuracy is maintained (less than 2% error) for surface angles up to this limit.

In more practical application, the instrument's abilities were exhibited by experimental thickness data

for shear-driven and gravity-driven films. Comparing both cases supported the conclusion that the LFD instrument can be properly utilized for time-averaged film thickness measurements even for the case of shear-driven liquid films, where time-resolved data is incomplete. Therefore, the LFD instrument can be effectively utilized as a fluid dynamics tool with potential for improvement. The instrument's limitations can be improved by altering geometrical design of a given LFD measuring unit. For example, the maximum measurable surface angle can be directly increased by increasing the laser cone angle, θ_c. Although LFD instruments with maximum measurable surface angles of less than 10º have been successfully used for fluid measurements, experimentalists stand to gain from a larger maximum.

References

[1] S. Wittig, J. Himmelsbach, B. Noll, H. J. Feld, and W. Samenfink, "Motion and Evaporation of Shear-driven Liquid Films in Turbulent Gases," *J. of Engineering for Gas Turbines and Power*, Vol. 114, pp. 395-400, 1992.

[2] P. W. James, B. J. Azzopardi, Y. Wang, and J. P. Hughes, "A Model for Liquid Film Flow and Separation in a Wave-plate Mist Eliminator," *J. of Chemical Engineering Research and Design*, Vol. 83, pp. 469-477, 2005.

[3] G. F. Hewitt,, Measurement of Two Phase Flow Parameters, London: Academic Press, Inc., pp. 111-116, 1978.

[4] T. Takamasa and K. Kobayashi, "Measuring Interfacial Waved on Film Flowing Down Tube Inner Wall using Laser Focus Displacement Meter," *International J. of Multiphase Flow*, Vol. 26, pp. 1493-1507, 2000.

[5] T. Takamasa and T. Hazuku, "Measuring Interfacial Waves on Film Flowing Down a Vertical Plate Wall in the Entry Region using Laser Focus Displacement Meters," *International J. of Heat and Mass Transfer*, Vol. 43, pp. 2807-2819, 2000.

[6] S. Busam, J. Ebner, and S. Wittig, "An Experimental Study of Liquid Film Thickness in Annular Air/Oil Flow in a Vertical Pipe using a Laser Focus Displacement Meter," Presented at the *International Gas Turbine and Aeroengine Congress and Exhibition*, New Orleans, Louisiana, 2001.

[7] T. Hazuku, and N. Fukamachi, "Measurement of Liquid Film in Microchannels using a Laser Focus Displacement Meter," *Experiments in Fluids*, Vol. 38, pp. 780-788, 2005.

[8] T. Hazuku, T. Takamasa, T. Hibiki, and M. Ishii, "Interfacial Area Concentration in Annular Two-phase Flow," *International J. of Heat and Mass Transfer*, Vol. 50, pp. 2986-2995, 2007.

[9] T. Hazuku, T. Takamasa, and Y. Matsumoto, "Experimental Study on Axial Development of Liquid Film in Vertical Upward Annular Two-phase Flow," *International J. of Multiphase Flow*, Vol. 34, pp. 111-127, 2008.

[10] E. T. Hurlburt and T. A. Newell, "Optical Measurement of Liquid Film Thickness and Wave Velocity in Liquid Film Flows," *Experiments in Fluids*, Vol. 21, pp. 357-362, 1996.

[11] E. Hecht, Theory and Problems of Optics, McGraw Hill Book Co., pp. 40-41, 1975.

[12] T. J. Love, Radiative Heat Transfer, C.E. Merrill Publishing Co., pp. 55-68, 1968.

[13] H. Lan, J. L. Wegener, B. F. Armaly, and J. A. Drallmeier, "Developing Laminar Gravity-driven Film Flow down an Inclined Plane," Submitted to the Journal of Fluids Engineering, 2009.

[14] M. A. Friedrich, H. Lan, J. L. Wegener, J. A. Drallmeier, and B. F. Armaly, "A Separation Criterion with Experimental Validation for Shear-driven Films in Separated Flows," *J. of Fluids Engineering*, Vol. 130, Issue 5, 051301, 2008.

[15] J. L. Wegener, M. A. Friedrich, J. A. Drallmeier, and B. F. Armaly, "Experimental Evaluation of a Film Separation Criterion," *Proceedings of the 11th Triennial International Conference on Liquid Atomization and Spray Systems*, Vail, Colorado USA, July 2009.

Acknowledgements

This work was supported in part by NSF grant CTS-0352135.

Nomenclature

- A laser beam cross sectional area
- h thickness
- $\bar{h}$ mean thickness
- U_g gas phase velocity
- θ_c laser beam cone angle

ρ reflection coefficient
σ standard deviation
R laser beam radius
P power of incident light
P_o power of reflected light
α surface angle
θ angle between ray of light and optical axis
n refractive index
m complex refractive index
k imaginary part of refractive index
z spanwise direction

Subscripts
$\perp$ perpendicular
$//$ parallel
1 incident
2 reflected
s sapphire
al aluminum
a air
w water
f film